[12]J. C. Slater, Phys. Rev. **81**, 385 (1951).
[13]L. Kleinman and R. Shurtleff, Phys. Rev. **188**, 1111 (1969).
[14]Tables similar to Table I may be obtained from the authors for the Z and A points.
[15]J. C. Slater and G. F. Koster, Phys. Rev. **94**, 1498 (1954).
[16]R. Shurtleff and L. Kleinman, Phys. Rev. B **3**, 2418 (1972).
[17]In order to avoid confusion when we talk about hybridized p-d bands we shall refer to the bands which are O_{2p} and V_{3d} in the tight-binding limit as valence and conduction bands, respectively.
[18]D. W. Fischer, Phys. Rev. B **5**, 4219 (1972).
[19]J. B. Goodenough, J. Solid State Chem. **3**, 490 (1971).
[20]J. W. Pierce and J. B. Goodenough, Phys. Rev. B **5**, 4104 (1972).
[21]E. B. Caruthers and L. Kleinman, following paper, Phys. Rev. B 7, 3760 (1973).

PHYSICAL REVIEW B VOLUME 7, NUMBER 8 15 APRIL 1973

Energy Bands of Semiconducting VO_2†

Ed Caruthers and Leonard Kleinman
Department of Physics, University of Texas, Austin, Texas 78712
(Received 30 October 1972)

For $T > T_t \simeq 68°$ C, VO_2 is a metal with the rutile structure. For $T < T_t$, VO_2 is a semiconductor with a monoclinic structure. We have found semiconducting energy bands for the low-temperature structure from a parametrized tight-binding linear-combination-of-atomic-orbitals calculation. The semiconducting gap results not only from the reduced symmetry of the monoclinic phase but also from changes in the tight-binding parameters which result from changed interatomic distances. The joint density of states derived from our calculation is in very good agreement with experimental optical data. The success of this calculation shows that, given the crystal structure, the semiconducting band gap is completely understandable in terms of one-electron theory. A short Appendix on the group theory of this structure is included.

I. INTRODUCTION

VO_2 undergoes a first-order phase transition at $T_t = 68$ °C from a monoclinic semiconductor ($T < T_t$) to a tetragonal metal ($T > T_t$). Phase transitions characterize several oxides of vanadium, and the general class of transition-metal oxides shows a wide range of magnetic and electrical properties. All these oxides contain a distinct conduction band, arising from metal nd atomic orbitals, which is above a valence band of O_{2p} states and below the band of metal $(n+1)s$ states. In the case of VO_2, the $3d^3 4s^2$ vanadium atoms contribute four electrons each to fill the valence band. This leaves one electron per vanadium ion in the conduction band. Since there are an even number of vanadium atoms in the unit cell (V_2O_4 for $T > T_t$, V_4O_8 for $T < T_t$), the semiconducting state must be characterized by a gap separating completely filled bands of $3d$ states from all the higher-energy $3d$ states. A great deal of work has been devoted to the problems of how the band gap arises from the phase transition, and what the mechanism is which drives the transition.[1,2]

In principle the investigation of VO_2 should include completely self-consistent band calculations, using nonspherical potentials, performed on both the high- and low-temperature phases. The detailed energy bands would facilitate interpretation of optical and photoemission experiments. The differences in the charge density of the two phases would greatly aid explanation of the transition, as would changes in the various components of the binding energy. Unfortunately, this sort of calculation is not technically feasible for VO_2. The high-temperature phase has a tetragonal unit cell containing two formula weights of VO_2 (rutile structure). In our investigation of this phase[3] we found that the large size of the unit cell relative to the augmented-plane-wave (APW) spheres made 350–400 APWs necessary for the expansion of the wave functions. Since there are 12 filled valence bands and ten conduction bands (five of which are partially occupied), the calculation of charge density necessary for a self-consistent calculation was not possible. The low-temperature phase has a monoclinic space group with four formula weights of VO_2 in the unit cell, and is even less amenable to exact calculation.

The purpose of this paper is to present a first approximation to the energy bands of semiconducting VO_2. In order to show how the band gap arises from the changes in crystal symmetry, we have performed a parametrized tight-binding linear-combination-of-atomic-orbitals (LCAO) calculation on the monoclinic crystal structure. Our method was to begin with all tight-binding parameters (TBPs) that were the same as those which produced

TABLE I. Atomic positions for VO_2 in rutile and monoclinic structures. All coordinates are given in terms of the tetragonal primitive translations $\vec{a}_r = a_r\hat{x}$, $\vec{b}_r = a_r\hat{y}$, $\vec{c}_r = c_r\hat{z}$.

	Rutile structure		Monoclinic structure
(V)	(0.305, 0.305, 0.000)	⟷	(0.315, 0.325, −0.041)
(I)	(0.000, 0.000, 0.000)	⟷	(0.000, 0.000, 0.000)
(VI)	(−0.305, −0.305, 0.000)	⟷	(−0.285, −0.265, −0.031)
(VII)	(0.305, 0.305, 1.000)	⟷	(0.335, 0.315, 0.949)
(II)	(0.000, 0.000, 1.000)	⟷	(0.050, 0.050, 0.918)
(VIII)	(−0.305, −0.305, 1.000)	⟷	(−0.265, −0.275, 0.959)
(IX)	(−0.805, −0.195, 0.500)	⟷	(−0.765, −0.175, 0.459)
(III)	(−0.500, −0.500, 0.500)	⟷	(−0.450, −0.500, 0.500)
(X)	(−0.195, −0.805, 0.500)	⟷	(−0.165, −0.765, 0.469)
(XI)	(0.805, −0.805, −0.500)	⟷	(0.815, −0.775, −0.541)
(IV)	(0.500, −0.500, −0.500)	⟷	(0.500, −0.450, −0.582)
(XII)	(0.195, −0.195, −0.500)	⟷	(0.215, −0.185, −0.551)

the high-symmetry energy bands. We then looked for changes in the TBPs which would be consistent with the changes in interatomic distances which result from the metal-semiconductor phase transition. Our goal was to find changes in the parameters which would produce bands agreeing with experimental information about the semiconducting phase. Before discussing the parameter changes and the bands, we will review briefly the experimental information about semiconducting VO_2.

The crystal structure for room-temperature VO_2 was first determined by Andersson[4,5] in 1954. In 1961 Westman[6] determined the relations between the high- and low-temperature phases, and we will use these relations to describe the low-temperature monoclinic phase in terms of the high-temperature tetragonal phase. We have found that this makes the less symmetric structure easier to visualize. V_2O_4 (rutile structure) has the following primitive translation vectors:

$$\vec{a}_r = a_r\hat{x}\ ,\quad \vec{b}_r = a_r\hat{y}\ ,\quad \vec{c}_r = c_r\hat{z}\ ,$$

where $a_r = 4.530$ Å and $c_r = 2.869$ Å. Here the subscript r denotes rutile structure, and $\hat{x}$, $\hat{y}$, and $\hat{z}$ denote the usual rectangular unit vectors. V_4O_8 (monoclinic structure) has as its primitive translation vectors $\vec{a} = 5.743$ Å, $\vec{b} = 4.517$ Å, and $\vec{c} = 5.375$ Å, where the angle between $\vec{a}$ and $\vec{c}$ is $\beta = 122.61°$. To within experimental accuracy, the unit cells are related by $\vec{a} = 2\vec{c}_r$, $\vec{b} = \vec{a}_r$, $\vec{c} = \vec{b}_r - \vec{c}_r$. If there is any volume change, it is less than 1%, and it is neglected in our calculations. We note here that $|\vec{a} + \vec{c}| = |\vec{c}|$, so that the hexagonal base of the unit cell (perpendicular to the $\hat{x}$ axis) shows reflection symmetry in the $z = 0$ and $y = 0$ planes. But the actual crystal has lower symmetry than this, due to the arrangement of atoms within the unit cell. In Table I are given the atomic positions for both the rutile and the monoclinic structures. All coordinates for both structures are given in terms of the rutile axes $\vec{a}_r$, $\vec{b}_r$, $\vec{c}_r$. (I)–(IV) denote vanadium positions; (V)–(XII) denote oxygen positions.

The monoclinic phase has a center of inversion at (0.025, 0.025, 0.459), midway between the vanadium atoms (I) and (II). The four symmetry operations at this point are E, the identity; II, the inversion; $\{\sigma_b \mid \tau\}$, a glide plane involving a reflection in the plane perpendicular to $\vec{b}$ followed by a translation $\vec{\tau} = \frac{1}{2}(\vec{b} + \vec{c}) = (\frac{1}{2}, \frac{1}{2}, -\frac{1}{2})$; and $\{C_2 \mid \tau\}$, a screw axis consisting of a rotation of π about a line parallel to $\vec{b}$ followed by the translation $\vec{\tau}$. There is no reflection symmetry in the plane containing $\vec{a}$ and $\vec{b}$. The space group is, therefore, $C_{2h}^5(P2_1/c)$.

The most prominent feature of the phase transition is that the nearest-neighbor vanadium atoms which are spaced equidistantly along the $\vec{c}_r$ in the rutile structure pair up and depart slightly from collinearity in the monoclinic structure. The distance between (I) and (II) is 2.65 Å, while the distance between (I) and (II-$\vec{a}$) is 3.12 Å. Thus the TBPs for vanadium atoms a distance 2.869 Å apart in the rutile structure must be replaced by two sets of TBPs in the monoclinic structure: one for vanadium atoms 2.65 Å apart and one for vanadium atoms 3.12 Å apart. Another feature of the transition is the increased distortion of the octahedron formed by each vanadium atom's six nearest oxygen neighbors. In the rutile structure, the vanadium at (0, 0, 0) has oxygen neighbors at (0.305, 0.305, 0.000), (−0.305, −0.305, 0.000), (0.195, −0.195, 0.500), (0.195, −0.195, −0.500), (−0.195, 0.195, −0.500), and (−0.195, 0.195, 0.500). The first two are 1.95 Å away and the last four are 1.90 Å away. In the monoclinic structure, these oxygen neighbors shift to the positions (0.315, 0.325, −0.041), (−0.285, −0.265, −0.031), (0.235, −0.175, 0.459), (0.215, −0.185, −0.551), (−0.165, 0.235, −0.531), and (−0.185, 0.225, 0.459). Their respective distances from the central vanadium atom are 2.05, 1.763, 1.87, 2.04, 2.01, and 1.865 Å. The $V_{(I)}$-$O_{(VI)}$ pair form an electric dipole. The $V_{(II)}$-$O_{(VII)}$ pair form a similar dipole, oriented in exactly the opposite direction. Thus we can look upon the phase change as shifting the vanadiums away from the centers of their oxygen octahedra in such a way as to produce antiferroelectric ordering along the $\vec{c}_r$ axis. As first emphasized by Heckingbottom and Linett,[7] there is a greater percent decrease in the $V_{(I)}$-$O_{(VI)}$ distance than in the $V_{(I)}$-$V_{(II)}$ distance. We therefore expect that the parameters affected by the changes in (I)-(II) and (I)-(VI) distances will have the largest effects in producing the band gap.

The reciprocal-lattice vectors are

$$\vec{K}_1 = (2\pi/a_r)\hat{x}\ ,\quad \vec{K}_2 = (2\pi/a_r)\hat{y}\ ,\quad \vec{K}_3 = (\pi/a_r)\hat{y} + (\pi/c_r)\hat{z}\ .$$

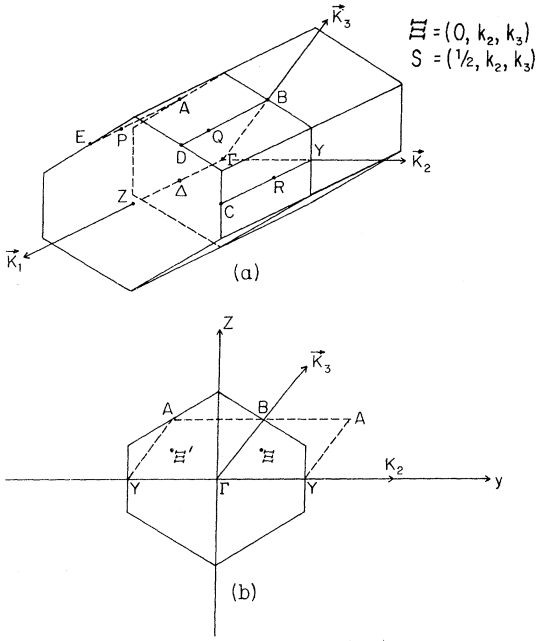

FIG. 1. (a) First Brillouin zone for the monoclinic structure of VO_2. (b) The $k_1 = 0$ plane of the zone shown in (a).

An arbitrary $\vec{k}$ vector will be denoted (k_1, k_2, k_3), such that

$$\vec{k} = 2\pi[(k_1/a_r)\hat{x} + (k_2/a_r + \tfrac{1}{2}k_3/a_r)\hat{y} + \tfrac{1}{2}(k_3/c_r)\hat{z}] , \tag{1}$$

and an arbitrary real-space vector $\vec{r}$ will be denoted (x, y, z) such that

$$\vec{r} = xa_r\hat{x} + ya_r\hat{y} + zc_r\hat{z} . \tag{2}$$

Thus

$$\vec{k}\cdot\vec{r} = 2\pi[k_1x + (k_2 + \tfrac{1}{2}k_3)y + \tfrac{1}{2}k_3z] . \tag{3}$$

Figure 1(a) shows the first Brillouin zone for this structure, labeled according to Zak's notation.[8] We note that it appears more symmetric than most monoclinic Brillouin zones because the y component of $\vec{K}_3$ is exactly $\frac{1}{2}$ of $\vec{K}_2$. Of course, there is no reflection symmetry through the $y = 0$ or $z = 0$ planes. The crystal wave function will have different values at the two $\vec{k}$ points Ξ and Ξ′. Because of the symmetry operations, $\frac{1}{4}$ of the Brillouin zone will contain all the independent values of $\vec{k}$. We could work with the part of the Brillouin zone above the y axis in Fig. 1(b), but we prefer to work with the equivalent section enclosed by the dashed lines. Our quarter zone is, therefore, defined by

$$0 \le k_1 \le \tfrac{1}{2} , \quad -\tfrac{1}{2} < k_2 \le \tfrac{1}{2} , \quad 0 \le k_3 \le \tfrac{1}{2} .$$

The group theory for the rutile space group has been done by Gay, Albers, and Arlinghaus,[9] but as far as we know the group theory for this monoclinic structure has not previously been published. Zak[8] presents correct character tables, but the points with which they are associated are often incorrect. We, therefore, include a short appendix on this.

Experimental information is less complete in its description of the energy bands than in its description of the crystal structure. Ideally, we would like to know the widths of the (filled) valence $3d$ bands and the (empty) conduction $3d$ bands, the widths of the gaps between the valence $3d$ bands and the $3d$ bands above and the $2p$ bands below, and the width of the $2p$ bands. But to get even a part of this information requires careful consideration of several different types of experiments, each of which provides incomplete information.

Powell, Berglund, and Spicer[10] have performed photoemission experiments on both metallic and semiconducting samples of VO_2. Their semiconducting quantum-yield curve is a near perfect duplicate of the metallic curve, except that it is shifted 0.6 eV toward higher energy. The high-energy intercepts of the energy distribution curves (EDCs) are 0.6 eV higher in the semiconducting case for a given photon energy than they are in the metallic case. The authors conclude that all the occupied V_{3d} and O_{2p} states are moved about 0.6 eV downward relative to the Fermi level. Spicer[11] and Derbenwick[12] consider that the sample was probably heavily doped n type, so that the band gap is not much more than 0.6 eV. Derbenwick's photoemission experiments[12] found the top of the valence band to be 0.1–0.3 eV below the Fermi level, depending on the sample, possibly implying acceptor impurities in his samples. But Derbenwick also suggests that the size of the band gap may be a function of stoichiometry with poorer crystals having small band gaps.

Optical experiments have been performed by Derbenwick,[12] Verleur, Barker, and Berglund,[13] Gavini and Kwan,[14] and by Ladd.[15] All show a low-energy peak in the reflectivity at about 1 eV, attributed to d-d transitions, and a double peak around 2.8 and 3.6 eV, attributed to p-d interactions. The p-d peaks are at the same energy in the semiconductor as in the metal. This indicates that the O_{2p} states in the semiconductor have not moved to a lower energy than they had in the metal, as has been suggested from photoemission data.[10] Derbenwick's optical data extend over the widest range of photon energies and are consistent with an O_{2p} bandwidth of 6–8 eV, in contrast to estimates of a 3-eV (Ref. 10) or 5-eV (Ref. 12) bandwidth from photoemission data. Unfortunately, none of the optical data shows a low-energy cutoff for $\hbar\omega = E_g$, the width of the band gap. For example, Verleur *et al.* reported that their optical ab-

sorption coefficient increased steadily from a value of 10^3 cm^{-1} at $\hbar\omega = 0.2$ eV to 10^5 cm^{-1} for $\hbar\omega = 1.0$ eV, providing absolutely no information about the band gap. The work of Gavini and Kwan shows a somewhat more structure, especially in their graph of the imaginary part of the dielectric constant ϵ_2. Though this goes to zero only at $\hbar\omega = 0$, there is a sharp increase in slope for $\hbar\omega > 0.6$ eV. We interpret this increase in slope as due to the onset of direct transitions, and we think that the low-energy tail is due to transitions from impurity states and to departures from stoichiometry. This plus the ambiguity in the photoemission data supports the conclusion of Berglund and Guggenheim[16] that there are a variety of traps and defect states whose distribution through the band gap depends on the sample. Estimates[17] of a low-temperature activation energy of 0.15 eV from extrapolation of the dc conductivity are almost certainly due to impurity states. We have, therefore, worked to produce bands with a semiconducting gap of about 0.6 eV.

II. ENERGY BANDS

To find energy bands for the monoclinic structure of VO_2, we have used a basis set of 56 Bloch functions made from the 20 V_{3d} orbitals, the 24 O_{2p} orbitals, the 4 V_{4s} orbitals, and the 8 O_{3s} orbitals within the unit cell. Matrix elements between basis functions are expressed as a sum of geometrical factors times TBPs according to the method of Slater and Koster.[18] For purposes of obtaining the geometrical relations, these parameters are taken to have the symmetry of σ, π, or δ molecular orbitals between atoms a given distance apart. In principle, a different set of parameters is necessary for each different interatomic separation. In the rutile structure, this presented no problem, and all near-neighbor interactions were included in a set of 44 parameters.[3] However, there are so many changes in interatomic distances in passing to the monoclinic phase that 140 TBPs are in principle necessary to describe the same interactions. It is not feasible to do an APW calculation in this structure and there are certainly not enough experimentally known features of the energy bands to permit fitting of all the TBPs.

We have, therefore, treated the TBPs as a set of disposable constants. As a first approximation to the correct set, we kept the parameters for every interaction the same as they were in the high-symmetry case. For instance, the same $dd\sigma$, $dd\pi$, and $dd\delta$ were used to describe the (I)-(II) and the (I)-(II-$\vec{a}$) interactions that were used to describe the (I)-(II) interactions in the rutile structure. This did not produce a band gap, but it did provide a starting point. Since our results for the metallic case showed that the lowest V_{3d} levels depend primarily on the pd and dd parameters, we did not change any of the O_{2p}-O_{2p}, V_{4s}-V_{4s}, O_{3s}-O_{3s}, V_{3d}-V_{4s}, V_{3d}-O_{3s}, O_{2p}-V_{4s}, or O_{2p}-O_{3s} parameters. We increased the strength of pd and dd interactions if the neighbors moved closer together during the metal-semiconductor transition and we decreased the interaction where neighbors moved further apart. Typical changes were the multiplication of $(dd\sigma)_{\text{I-II}}$ by 20, $(pd\pi)_{\text{I-VI}}$ by 15, $(pd\pi)_{\text{I-VII,IX}}$ by 1.5, $(pd\sigma)_{\text{I-VII,IX}}$ by 1.5, $(pd\sigma)_{\text{I-VI}}$ by 1.0, and $(dd\delta)_{\text{I-II}}$ by 10. Since the $(dd\sigma)_{\text{I-II}}$ parameter was originally 50 times smaller than the $pd\sigma$ parameters, the factor of 20 does not make a large absolute change. The multiplicative factors for neighbors moved further apart in the transition ran from 0.7 to 0.4.

Our energy bands are presented in Fig. 2. There is a slight overlap of the V_{3d} valence band with the O_{2p} band, but no crossings at any point in the Brillouin zone. The actual maximum in the V_{3d} valence band is -0.8116 Ry at (0, -0.3750, 0.2143). The minimum in the conduction band is -0.7671 Ry at (0, 0.315, 0.5), so that the total indirect gap is 0.0445 Ry or 0.6052 eV. The minimum direct gap is 0.0471 Ry or 0.6406 eV at (0, 0.3125, 0.5). We note that the bottom of our conduction band is very flat, implying a large effective mass for electrons. This supports Paul's estimate from Boltzmann transport expressions of $m^* \approx 100 m_0$,[19] better than Berglund and Guggenheim's[16] estimates of $1.6 m_0 \leq m^* \leq 7 m_0$ from conductivity and Hall-effect data and $m_0 \leq m^* \leq 4 m_0$ from optical data. Since our bands predict a lower effective mass for holes than for electrons, we expect p-type conductivity for intrinsic crystals. So far, Hall-effect and thermopower measurements have indicated conduction by electrons only, but as indicated above, most samples seem to be extrensic. Ladd has argued[15] that the low Hall constant and short mean free path (about 20% of the average vanadium-vanadium spacing) deduced from transport data can be most plausibly explained as the result of both electron and hole contributions to conductivity.

Both our density of states (presented in Fig. 3) and our joint density of states were obtained from eigenvalue calculations at 3584 $\vec{k}$ points (1026 independent points). The widths of the p and d bands have increased by 20% relative to the metallic density of states, and deep gaps which were not present in the metal have appeared. The increases in bandwidths resulted primarily from the large increase in $(pd\pi)_{\text{I-VI}}$, even though the bottom of the O_{2p} band and the top of the V_{3d} band are much more sensitive to changes in $(pd\sigma)_{\text{I-VI}}$. We could not have increased the latter parameter without greatly increasing the bandwidths. We have divided the joint density of states $J(E)$ by E^2 and we present

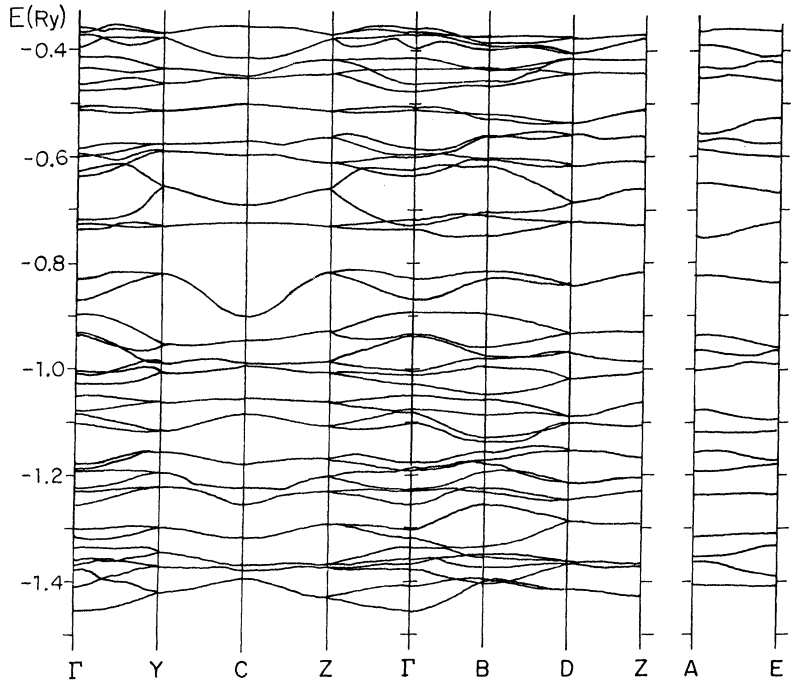

FIG. 2. Energy bands of monoclinic VO_2 plotted along principal symmetry directions. Points of high symmetry are labeled as in Fig. 1.

the result in Fig. 4 along with graphs of the imaginary part of the dielectron constant ϵ_2. In the random-phase approximation, at zero temperature, ϵ_2 is proportional to

$$\frac{1}{E^2}\sum_{m,n}\int |M_{mn}|^2\delta(E_n - E_m - E)d\vec{k}\,, \tag{4}$$

where m labels occupied states, n labels unoccupied states, and the interband oscillator strength is

$$M_{nm}(\vec{k}) = -(i/\Omega)\int \psi^*_{\vec{k}m}\nabla\psi_{\vec{k}n}d\Omega\,, \tag{5}$$

with Ω the volume of the unit cell. Since $J(E)$ is proportional to

$$\sum_{m,n}\int \delta(E_n - E_m - E)d\vec{k}\,,$$

we expect $J(E)/E^2$ to be proportional to ϵ_2 as long as the matrix elements remain fairly constant. The main difference between theory and experiment is in the height of the peak near 1 eV. This peak is due to d-d transitions which would be forbidden in atomic systems. It is, therefore, reasonable to expect that the matrix elements would reduce the height of this first peak relative to the

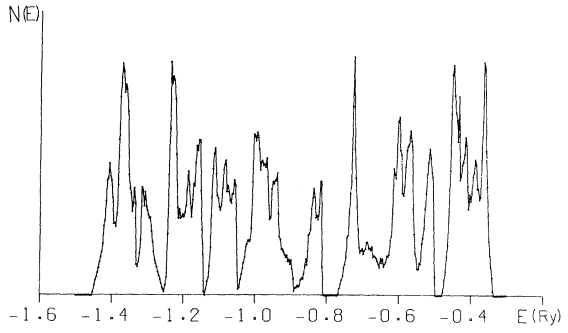

FIG. 3. Density of states for monoclinic VO_2. Units of $N(E)$ are arbitrary. The gap at -0.8 Ry lies within the vanadium d bands and makes the material a semiconductor.

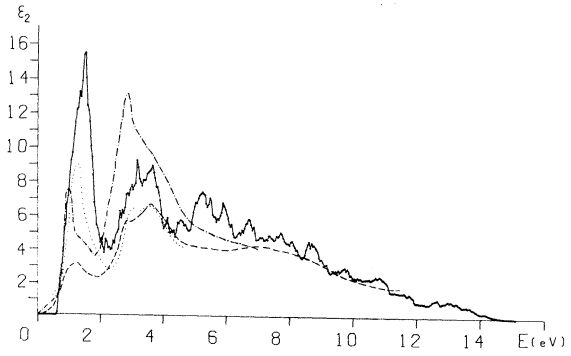

FIG. 4. The dotted curve, the dashed curve, and the dot-dashed curve all show ϵ_2 derived from optical experiments on semiconducting VO_2. The sources of the curves are, respectively, J. C. C. Fan, Office of Naval Research Technical Report Nos. HP-28 and ARPA-43, 1972 (unpublished), Ref. 12, and Ref. 14. The solid curve shows our calculation of $J(E)/E^2$ and is scaled to fit on the graph with the other curves.

rest of the graph. In fact, Derbenwick[12] has concluded from his photoemission data that states in the O_{2p} band couple 2.5 times more strongly with the vacuum level than do states in the V_{3d} valence band. If we assume that the same ratio holds for optical transitions, the height of the first peak is reduced to 6.2, in good agreement with the experimental curves.

III. DISCUSSION

It has been known since 1959[20] that there is a semiconductor-metal transition. Since 1961[6] it has been known that this coincides with the structural transition from monoclinic to tetragonal. It is now possible to provide quantitative support for Goodenough's 1971 model[2] of how the phase change and the conductivity change are coupled: First, the decreased $V_{(I)}$-$O_{(VI)}$ distance increases the $pd\pi$ parameter between these neighbors. In the language of molecular-orbital theory, this makes $pd\pi$ bonding levels more stable and $pd\pi$ antibonding levels less stable. Goodenough postulates four vanadium-vanadium orbitals left at the bottom of the V_{3d} band as a result of the upward movement of the $pd\pi$ antibonding levels. We found that after changing the pd parameters, and before changing the dd parameters, the four lowest V_{3d} levels at Γ were composed primarily of $d_{3z^2-r^2}$ with some admixture of d_{xy}. The reduced symmetry of the monoclinic phase is not enough to produce a band gap without changes in the dd parameters, but the changes in parameters produced by the decreased $V_{(I)}$-$V_{(II)}$ distance do produce the gap shown in Figs. 2 and 3. Since Goodenough originally suggested[21] that the semiconduction might result just from the formation of localized bonds between pairs of vanadium atoms clustered together along the $\vec{c}_r$ axis, we also attempted to produce a band gap by only varying the dd parameters. We were only able to do this by increasing $(dd\sigma)_{I\text{-}II}$ to 105 times its metallic value. The resulting bands[22] showed a direct gap of 0.645 eV, but the indirect gap was only 0.188 eV. These bands also did not show the double peak in $J(E)/E^2$ between 2.5 and 4.0 eV. We therefore conclude that changes in the p-d interaction play an essential part in the production of the band gap.

Even now it is not possible to be sure why the phase transition occurs. We know that above T_t the free energy, $F = E - TS$, must be lower for the metallic structure than for the semiconducting structure, and we know that for $T < T_t$ the monoclinic structure must have the lower F. But we cannot calculate the temperature dependence of either E or S, and we cannot say whether it is changes in E or in S which predominate at T_t. That is, we cannot tell whether the material changes from semiconductor to metal in order to lower the electronic energy, or whether the change in conductivity is the effect of a structural change maximizing the phonon contribution to S and possibly occurring in spite of an increase in the electronic energy. The fact that the calculation of Adler and Brooks[23] predicts a transition temperature of about 870 °K (for an energy gap of 0.6 eV) on the basis of electronic energies alone would seem to indicate that at 68 °C the electronic energy is still higher in the metallic state than in the semiconducting state. However, there are many simplifying assumptions which go into this model, and no calculations have been done which would

TABLE II. General multiplication table for any $\vec{k}$ point having all four symmetry operations in its group.

	E	Π	σ	C
E	E	Π	σ	C
Π	Π	E	C	σ
σ	σ $\{C \mid (-1, -1, 1)\}$	$\{E \mid (0, 1, -1)\}$	$\{\Pi \mid (1, 0, 0)\}$	
C	C $\{\sigma \mid (-1, -1, 1)\}$	$\{\Pi \mid (0, 1, -1)\}$	$\{E \mid (1, 0, 0)\}$	

TABLE III. Multiplication tables and irreducible representations for eight points of high symmetry.

Γ, B	E	Π	σ	C
E	E	Π	σ	C
Π	Π	E	C	σ
σ	σ	C	E	Π
C	C	σ	Π	E

	E	Π	σ	C
Γ_1, B_1	1	1	1	1
Γ_2, B_2	1	−1	−1	1
Γ_3, B_3	1	1	−1	−1
Γ_4, B_4	1	−1	1	−1

Y, A	E	Π	σ	C
E	E	Π	σ	C
Π	Π	E	C	σ
σ	σ	$\bar{C}$	$\bar{E}$	$\bar{\Pi}$
C	C	$\bar{\sigma}$	$\bar{\Pi}$	$\bar{E}$

	E	Π	σ	C
Y_1, A_1	$\begin{pmatrix}1&0\\0&1\end{pmatrix}$	$\begin{pmatrix}0&1\\1&0\end{pmatrix}$	$\begin{pmatrix}0&1\\-1&0\end{pmatrix}$	$\begin{pmatrix}1&0\\0&-1\end{pmatrix}$

C, E	E	Π	σ	C
E	E	Π	σ	C
Π	Π	E	C	σ
σ	σ	C	$\bar{E}$	$\bar{\Pi}$
C	C	σ	$\bar{\Pi}$	$\bar{E}$

	E	Π	σ	C
C_1, E_1	1	1	i	i
C_2, E_2	1	−1	$-i$	i
C_3, E_3	1	1	$-i$	$-i$
C_4, E_4	1	−1	i	$-i$

Z, D	E	Π	σ	C
E	E	Π	σ	C
Π	Π	E	C	σ
σ	σ	$\bar{C}$	E	$\bar{\Pi}$
C	C	$\bar{\sigma}$	Π	$\bar{E}$

	E	Π	σ	C
Z_1, D_1	$\begin{pmatrix}1&0\\0&1\end{pmatrix}$	$\begin{pmatrix}0&-1\\-1&0\end{pmatrix}$	$\begin{pmatrix}1&0\\0&-1\end{pmatrix}$	$\begin{pmatrix}0&-1\\1&0\end{pmatrix}$

TABLE IV. Irreducible representations for the ΔP, Q, R, S, and Ξ points.

Δ, P, Q, R	E	$\{C_2 \mid \tau\}$	Ξ, S	E	$\{\sigma_b \mid \tau\}$
1	1	$e^{i\pi k_1}$	1	1	$e^{i\pi k_2}$
2	1	$-e^{i\pi k_1}$	2	1	$-e^{i\pi k_2}$

TABLE V. Compatibility relations.

Γ_1	Γ_2	Γ_3	Γ_4	B_1	B_2	B_3	B_4
Ξ_1	Ξ_2	Ξ_2	Ξ_1	Ξ_1	Ξ_2	Ξ_2	Ξ_1
Δ_1	Δ_1	Δ_2	Δ_2	Q_1	Q_1	Q_2	Q_2
C_1	C_2	C_3	C_4	E_1	E_2	E_3	E_4
S_1	S_2	S_2	S_1	S_1	S_2	S_2	S_1
R_1	R_1	R_2	R_2	P_1	P_1	P_2	P_2
Y_1		A_1		Z_1		D_1	
R_1, R_2		P_1, P_2		Δ_1, Δ_2		Q_1, Q_2	
Ξ_1, Ξ_2		Ξ_1, Ξ_2		S_1, S_2		S_1, S_2	

justify the assumption that S gets much larger in the metallic phase for $T \geq T_t$. [*Note added in proof.* Professor W. Paul has called to our attention a paper by C. J. Hearn, J. Phys. C 5, 1317 (1972), which professes to show that the phase transition is driven by the excess phonon entropy of the metal.]

Although we are unable to explain the cause of the phase transition, we have shown that given the phase transition one can explain the huge change in conductivity in VO_2 with simple one-electron band theory. It does not require the use of complicated many-electron correlation effects such as have been proposed[1] for this and other transitions.

APPENDIX: GROUP THEORY FOR $C_{2h}^5(P2_1/c)$

The general multiplication table for this space group, including lattice translations produced by repeated operations, is given in Table II. Here σ stands for $\{\sigma_h | \tau\}$ and C stands for $\{C_2 | \tau\}$, where $\vec{\tau} = (\frac{1}{2}, \frac{1}{2}, -\frac{1}{2})$. From this table and the form of $\vec{k} \cdot \vec{r}$ in Eq. (3) it follows that any two $\vec{k}$ points $(k_1, k_2, 0)$ and $(k_1, k_2, \frac{1}{2})$ will have isomorphous multiplication tables. All four operations are in the factor group for the $\vec{k}$ points Γ and B. For the surface points Y, A, C, E, Z, and D, there will be a group of eight elements consisting of these four operations with either an even or odd primitive translation. The multiplication tables for the surface groups will have the form

$$\begin{pmatrix} A & \bar{A} \\ \bar{A} & A \end{pmatrix},$$

the A part of which is all that we include in Table III. The points Δ, P, Q, and R have only the symmetry operations E and C in the group of the $\vec{k}$ point, and the points Ξ, $\vec{k} = (0, k_2, k_3)$, and S, $\vec{k} = (\frac{1}{2}, k_2, k_3)$, have only E and σ in the group of the $\vec{k}$ point. Irreducible representations for these points are given in Table IV. Because S is a surface point, it actually has a double group with the operations $\bar{E} = \{E | (1, 0, 0)\}$ and $\bar{\sigma} = \{\sigma | (1, 0, 0)\}$. The application of Herring's test[24] shows that there is an extra sticking together at all S points resulting from time reversal degeneracy. Herring's test also shows that the surface points R and P, which have double groups with the operations $\bar{E} = \{E | (0, 1, -1)\}$ and $\bar{C} = \{C | (0, 1, -1)\}$, have an extra sticking together from time-reversal degeneracy. Finally, compatibility relations are given in Table V.

†Research supported by Air Force Office of Scientific Research (AFSC) under Grant No. AF-AFOSR-72-2308.

[1]D. Adler, Essays Phys. **1**, 33 (1970).
[2]J. B. Goodenough, J. Solid State Chem. **3**, 490 (1971).
[3]E. Caruthers, L. Kleinman, and H. I. Zhang, preceding paper. Phys. Rev. B 7, 3753 (1973).
[4]G. Andersson, Acta Chim. (Budap.) **8**, 1599 (1954).
[5]G. Andersson, Acta Chim. (Budap.) **10**, 623 (1956).
[6]S. Westman, Acta Chim. (Budap.) **15**, 217 (1961).
[7]R. Heckingbottom and J. W. Linett, Nature (Lond.) **194**, 678 (1962).
[8]J. Zak, A. Casher, M. Glueck, and Y. Gur, *The Irreducible Representations of Space Groups* (Benjamin, New York, 1969).
[9]J. Gay, W. Albers, Jr., and F. Arlinghaus, J. Phys. Chem. Solids **29**, 1449 (1968).
[10]R. J. Powell, C. N. Berglund, and W. E. Spicer, Phys. Rev. **178**, 1410 (1969).
[11]W. E. Spicer (private communication).
[12]G. F. Derbenwick, Stanford Electronics Laboratory, Technical Report No. 5220-2, 1970 (unpublished).
[13]H. W. Verleur, A. S. Barker, Jr., and C. N. Berglund, Phys. Rev. **172**, 788 (1968).
[14]A. Gavini and C. C. Y. Kwan, Phys. Rev. B **5**, 3138 (1972).
[15]L. A. Ladd, Office of Naval Research, Technical Report Nos. HP-26 and ARPA-41, 1971 (unpublished).
[16]C. N. Berglund and H. J. Guggenheim, Phys. Rev. **185**, 1022 (1969).
[17]D. Adler, Solid State Phys. **21**, 1 (1968).
[18]J. C. Slater and G. F. Koster, Phys. Rev. **94**, 1498 (1954).
[19]W. Paul, Mater. Res. Bull. **5**, 691 (1970).
[20]F. J. Morin, Phys. Rev. Lett. **3**, 34 (1959).
[21]J. B. Goodenough, Phys. Rev. **117**, 1442 (1960).
[22]Energy bands or graphs of the densities of states for this case can be obtained from the authors.
[23]D. Adler and H. Brooks, Phys. Rev. **155**, 826 (1967).
[24]V. Heine, *Group Theory in Quantum Mechanics* (Pergamon, New York, 1960).